

MASS TRANSFER IN MEDIUM DENSITY FIBERBOARD (MDF) MODIFIED BY Na^+ MONTMORILLONITE (Na^+ MMT) NANOCCLAY

Reza Zahedsheijani¹, Hadi Gholamiyan¹, Asghar Tarmian¹, Hossein Yousefi¹

ABSTRACT

The potential use of nanoclay was examined to modify fluid transfer properties of medium density fiberboard (MDF). For this, Na^+ montmorillonite (Na^+ MMT) nanoclay was added to urea formaldehyde resin to produce MDF. Then, the air permeability and mass diffusivity of MDF were evaluated. Scanning electron microscope (SEM) images and X-ray diffraction (XRD) confirmed a dispersion and exfoliation of Na^+ MMT in the modified MDF. The air permeability presented a systematic decrease with increasing nanoclay amount. This reduction agreed with the simple “tortuous path” model. The nanoclay had no effect on the mass diffusivity.

Keywords: Air permeability, mass diffusivity, medium density fiberboard (MDF), Na^+ MMT nanoclay

INTRODUCTION

Medium density fiberboard (MDF) is widely used in the manufacturing of furniture, kitchen cabinets, door parts, panel moldings, laminate flooring and embossing. The world MDF capacity increased to 64.9 million m^3 in 2009 (Taylor *et al.* 2009). The future of MDF is dependent on the effort to improve its performance under service conditions and to decrease production costs (Walther *et al.* 2006). Like solid wood, MDF is a naturally hygroscopic material. It warps due to an asymmetrical density profile and relative humidity changes (Ganev *et al.* 2005a,b). Air permeability and mass diffusivity of wood and wood-based products are important parameters to predict their performance under service conditions. Thus, many investigations have been conducted to evaluate their mass transfer characteristics (Sorz and Hietz 2006; Straze and Gorisek 2006; Tarmian and Perre 2009). Moisture diffusion through the MDF panel can cause deformation, affecting the performance of final products, such as kitchen cabinet and furniture. The moisture diffusion model based on Fick's second law was found to be unsuccessful to determine the moisture absorption process in wood fiberboard and wood fiber/polymer composites (Shi 2007).

Nanotechnology represents a major opportunity for the forest products industry to develop new products. The nanotechnology searches to develop materials and structures that significantly improved physical and chemical properties and functions due to their nanoscale size (Wegner *et al.* 2005, Wegner and Jones 2006). At the present time, an increasing attraction is observed in the investigation of nanocomposite materials, comprising layered silicate clay. The important characteristics pertinent to application of clay minerals in polymer nanocomposites are their richest intercalation chemistry, high strength and stiffness and high aspect ratio of individual platelets, abundance in nature, low cost and high gas barrier quality (Zeng *et al.* 2005).

¹Department of Wood and Paper Science & Technology, Faculty of Natural Resources, University of Tehran, Karaj, Iran.
Received: 29.06.2010. Accepted: 26.03.2011
Corresponding author: Reza_zahed2009@ut.ac.ir

For gas barrier property, there are some papers in the literature. Initial studies of the effects of dispersed nanoclays into epoxy nanocomposite systems on gas permeability have been reported (Miller and Meador 2007). Those nanocomposites exhibited a reduction in gas permeability when compared to the neat resin. The nanoclays when separated and suitably dispersed in polymer are known to decrease the gas permeability of nanocomposites. The nanoclays are believed to increase the barrier properties, retarding the progress of gas molecules through the matrix resin (Ray and Okamoto 2003). The gas permeability of nanocomposites can be reduced by 70% using slight amount of nanoclay (Campbell *et al.* 2003). Actually, the small thickness and large aspect ratio as well as disk-like shape of the nanoclay create a “tortuous path” within the matrix for the gases to pass. The organomontmorillonite (OMMT)/polyurethane nanocomposite with high resistance to oxygen and water vapor permeation was investigated (Osman *et al.* 2003). The effect of nanoclay on gas permeability of polypropylene nanocomposite was also investigated by Pannirselvam *et al.* (2008). The author pointed out that the oxygen permeability of the nanocomposite decreased with increasing the nanoclay content. Rana (2003) showed that the montmorillonite nanoclay can decrease moisture diffusion through neat and glass fiber reinforced vinyl ester resin. In fact, the organoclay could improve the barrier performance of nanocomposites based on the simple “tortuous path” model. In the wood composite area of research, nanoclay was basically used for enhancement of mechanical properties (Ashori and Nourbakhsh 2009) and utilization of nanoclay for barrier quality of wood composite like MDF has not been investigated yet.

Our study was aimed to evaluate the effect of Na⁺ montmorillonite as nanofiller on the mass diffusivity and air permeability of MDF.

MATERIALS AND METHODS

Materials

Urea formaldehyde (UF) resin was used at level of 10% based on the oven-dry weight of wood fibers. The commercial UF resin was purchased from Tiran Chemie Inc., Karaj, Iran. The characteristics of the resin are given in table 1. Ammonium chloride (NH₄CL) was added as a hardener in UF resin at a level of 2% based on the oven-dry weight of resin. Na⁺ montmorillonite (Na⁺MMT) nanoclay with a cation exchange capacity (CEC) value of 92.6 mequiv/100 g was obtained from Southern Clay Products Inc., USA. The nanoclay was added to the resin at three levels of 0%, 2.5% and 5% based on the oven-dry weight of resin. The characteristics of Na⁺MMT nanoclay are given in Table 2. The wood fibers of Poplar (*Populus deltoides*) were kindly provided from the Arian Sina Inc., Sari, Iran. The final moisture content of the fibers after drying was about 1–2%. The dry fibers were classified using the Sonic Laboratory Sifter (VU100 type), Imal Inc., Italy. The average fiber length was 1.1 mm, and the amount of dust was close to 39.2%.

Table 1. The characteristics of UF resin based on laboratory tests.

Density (kg m ⁻³)	1300
Gel time (s)	69
Viscosity (CP)	320
pH	7
Solid amount (%)	60

Table 2. The characteristics of Na⁺MMT nanoclay based on Southern Clay Products Inc., USA.

Supplier designation	Cloisite [®] Na ⁺
Organic modifier	None
Density (kg m ⁻³)	2860
Moisture (%)	4–9
Weight loss on ignition (%)	7

Preparation of composites

MDF composites measuring 0.4×0.4×0.016 m³ with two densities of 650 and 750 kg m⁻³ were manufactured. The UF resin was mixed with the Na⁺MMT nanoclay by mechanical stirring for 360 s at the room temperature to get a good dispersion and partly exfoliation of Na⁺MMT in the UF resin (Lei *et al.* 2008). It seems the UF resin can also wet Na⁺MMT and partly penetrates into the silicate layers during this time. Then, the UF resin containing well-dispersed nanoclay was sprayed into the fibers by using a rotary blender. Mats were hand formed in a forming frame and then the fiber mats were manually pre-pressed. The fiber mats at 10% moisture content were exposed to the hot press. The hot press was applied at a pressure of 3.43×10⁶ Pa at 175°C for 360 s. Three replicate composites were made for each treatment. All composites were conditioned at 65±5% relative humidity and 20±1°C for about 2 weeks. The different prepared MDF trials are given in table 3.

Table 3. Amount of Na⁺MMT added and density of boards for the different MDFs

Code	Density of board (kg m ⁻³)	Na ⁺ MMT nanoclay (%)
A1		0
A2	650	2.5
A3		5
B1		0
B2	750	2.5
B3		5

X-ray diffraction (XRD)

Wide angle X-ray diffraction (WAXD) was applied to study the exfoliation of Na⁺MMT nanoclay in the structure of produced MDFs. The specimens were raw MDF, MDF containing 2.5% Na⁺MMT, MDF containing 5% Na⁺MMT and pure Na⁺MMT. The MDF specimens measuring 0.02×0.005×0.002 m³ were evaluated and three specimens from different parts of MDFs were used for each item. The XRD profile was detected by RINT-2000 diffractometer, Rigaku Inc., Japan (40000 V, 0.02 A) using Cu K α radiation ($\lambda=1.54073\text{\AA}$) at a scanning rate of 0.002° s⁻¹. We used a low scanning rate (0.002° s⁻¹) in order to decrease the ratio of noise/signal. The Cu K α radiation was irradiated on the specimen, perpendicular to the surface.

Measurement of air permeability (specific permeability)

Two cylindrical specimens (0.02 m in diameter and 0.015 m length) were prepared from medial and lateral parts each MDF randomly. The air permeability was measured perpendicular to the specimen’s surface. Therefore, the lateral surface of specimens was covered with epoxy resin to prevent any lateral flow of fluid. The length of specimens was 0.015 m because MDFs surface was cleaned with a razor blade. Figure 1 depicts a schematic of the experimental apparatus used for the air permeability measurement. This apparatus is traditionally used in many air permeability studies with few changes. This apparatus applies the falling water displacement method (Siau 1995) to measure the air permeability in specimens. All measurements were completed in a temperature-controlled room. The specific permeability (K) was calculated using Siau’s equations (Siau 1995, Parhizkari *et al.* 2010).

$$K = k_g \mu \tag{1}$$

where K is the specific permeability ($\text{m}^3 \text{m}^{-1}$), μ is the viscosity of air ($\mu=1.81 \times 10^{-5} \text{ Pa s}$) and k_g is the superficial permeability that can be determined as following.

$$k_g = \frac{V_d C L (P_{atm} - 0.074 \bar{z})}{t A (0.074 z) (P_{atm} - 0.037 z)} \times \frac{0.760 \text{ mHg}}{1.013 \times 10^5 \text{ Pa}} \tag{2}$$

where V_d is the volume of apparatus between points 1 and 2 [$V_d = \pi r^2 \Delta z$] (m^3), P_{atm} is the atmospheric pressure (m Hg), L is the length of MDF specimen (m), \bar{z} is the average height of water over surface of reservoir during period of measurement (m), A is the cross sectional area of MDF specimen (m^2), t is the time (s) and C is the correction factor for gas expansion as a result of change in static head and viscosity of water.

$$C = 1 + \frac{V_r (0.074 \Delta z)}{V_d (P_{atm} - 0.074 z)} \tag{3}$$

where V_r is the total volume of apparatus above point 1 [including volume of hoses] (m^3) and Δz is the change in height of water during time (m).

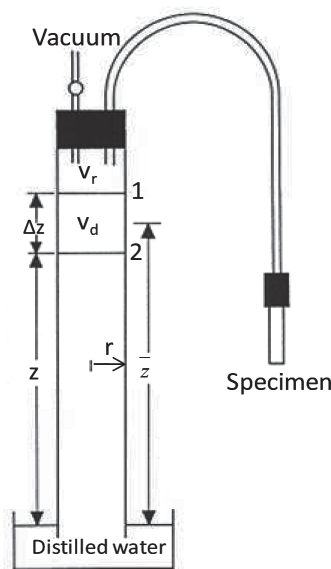


Figure 1. Schematic view of the air permeability measurement apparatus (from Siau 1995).

Measurement of moisture diffusion coefficient

The moisture diffusion coefficient was evaluated on the same specimens after the air permeability test (0.02 m in diameter and 0.01 m in length). The specimens back to the conditioning chamber at $65\pm 5\%$ relative humidity and $20\pm 1^\circ\text{C}$ between these two tests. The moisture diffusion coefficient test is time consuming. Therefore, we had to cut specimens at 0.01 m in length. The cup method was used to measure the moisture diffusion coefficient under a steady-state condition based on first Fick's law. The relative humidity (RH) inside the cup (75%) was controlled by using the saturated salt solution of sodium chloride. After preparation of the cups, they were placed inside a climatic chamber of 61% RH. Desorption followed at 20°C from 75% to 61% relative air humidity. Then, the moisture diffusivity was determined from the steady-state change in the cup weight vs. time after 19 days. The dimensionless diffusivity (f) can be determined by the following equation (Rousset *et al.* 2004).

$$f = \frac{Q}{D_v A} \times \frac{E}{(RH2 - RH1) \times P_{vs}(T)} \times \frac{RT}{M_v} \quad (4)$$

where D_v is the water vapor diffusion coefficient in air ($\text{m}^2 \text{s}^{-1}$), Q is the measured mass flow rate (kg s^{-1}), A is the cross section of specimen (m^2), E is thickness of the specimen (m), $RH1$ is the relative humidity inside the cup (%), $RH2$ is the relative humidity inside the climatic chamber (%), P_{vs} is the pressure of saturated water vapor (Pa), T is the temperature of the climatic chamber ($^\circ\text{K}$), R is the constant of perfect gas and M_v is the molar weight of vapor (kg mole^{-1}).

The dimensionless diffusivity (f) is the ratio between diffusion of water vapor in wood and diffusion of water-vapor in air (Rousset *et al.* 2004). It accounts for the resistance to the water-vapor migration due to the presence of wood compared to diffusion of vapor in the same layer of air; f is zero and one for a nondiffusive material and a diffusive material, respectively.

Field Emission Scanning Electron Microscopy (FE-SEM)

A vacuum dried thin layer of MDF containing Na^+MMT was coated with platinum by an ion sputter coater and was observed with a FE-SEM (JSM-6700F; JEOL Ltd., Tokyo, Japan) operating at 5000 V.

RESULTS AND DISCUSSION

X-ray diffraction analysis

Figure 2 shows the X-ray diffraction profile of pure Na^+MMT . It can be seen that Na^+ montmorillonite shows peaks at 7.3 , 14.45 , 20.05 , 21.05 , 26.86 , 28.8 , 35.11 , 43.79 , 54.31 and 62.35° . The peak at $2\theta=7.3^\circ$ is the strongest one that corresponds to a d-spacing of 1.21 nm according to Bragg's law (Faruk and Matuana 2008).

$$2d \sin \theta = n\lambda \quad (5)$$

where d is the spacing between planes, θ is half of the angle of diffraction, n is the order of diffraction ($n=1$) and λ is the X-ray wavelength ($\lambda=1.54073\text{\AA}$). Figure 3 shows the diffraction patterns for pure Na^+MMT , raw MDF, MDF containing 2.5% Na^+MMT and MDF containing 5% Na^+MMT in the range of $2\theta=3-12^\circ$. It can be seen that the strong peak of Na^+MMT at $2\theta=7.3^\circ$ disappeared completely in all MDF containing Na^+MMT which demonstrates that nanoclay were quite exfoliated and delaminated in UF resin. This shift of the XRD peak to lower value of 2θ indicates that the exfoliated structure was generated during the mixing and stirring of nanoclay with UF resin and within hot pressing of MDF. In fact, the sharp narrow diffraction peaks show crystalline structure of nanoclay, while the broad peak is amorphous structure after exfoliation. This finding is compatible with previous study (Lei *et al.* 2008) which reported that Na^+MMT is exfoliated when mixed with a UF resin. There are also several studies in the field of wood-based composites in which the exfoliation of nanoclay in the matrix was verified

(Ghasemi and Kord 2009, Lee *et al.* 2008, Lei *et al.* 2007). Actually, urea formaldehyde polymer chains could penetrate the galleries between clay layers hence, exfoliation took care.

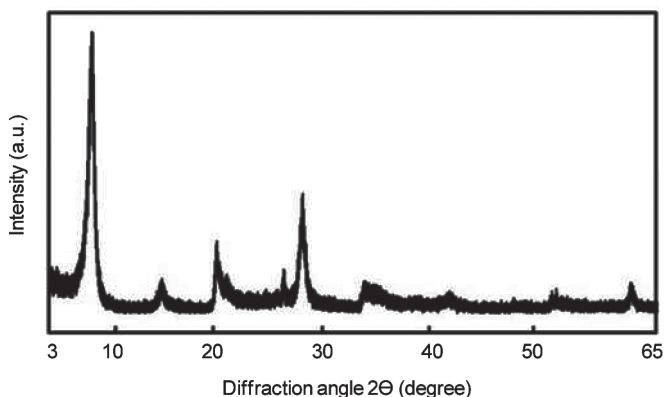


Figure 2. X-ray diffraction profile of pure Na⁺MMT

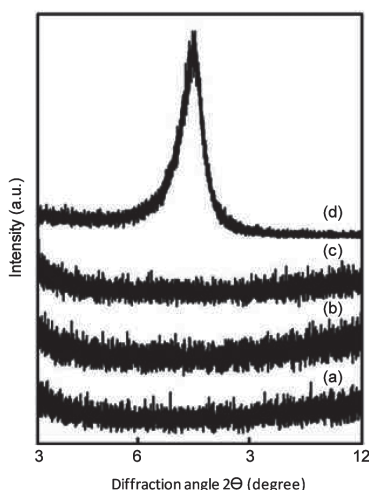


Figure 3. X-ray diffraction profiles of (a) raw MDF, (b) MDF containing 2.5% Na⁺MMT, (c) MDF containing 5% Na⁺MMT and (d) pure Na⁺MMT

Air permeability

Table 4 shows air permeability values for all 6 groups of specimens. The results show that all modified MDFs have less permeability values in comparison to control MDF, meaning a suitable barrier property in the modified MDFs. The air permeability value of control MDF (A1) is $13.8 \times 10^{-14} \text{ m}^3 \text{ m}^{-1}$, while that of MDFs treated with 2.5% and 5% of Na⁺MMT nanoclay (A2 and A3) is $13.7 \times 10^{-14} \text{ m}^3 \text{ m}^{-1}$ and $13.5 \times 10^{-14} \text{ m}^3 \text{ m}^{-1}$, respectively. Similarly, in the case of denser MDFs, the permeability value for B1 specimen is $3.62 \times 10^{-14} \text{ m}^3 \text{ m}^{-1}$, while the value for B2 and B3 specimens is $3.21 \times 10^{-14} \text{ m}^3 \text{ m}^{-1}$ and $2.75 \times 10^{-14} \text{ m}^3 \text{ m}^{-1}$, respectively. Similar to previous studies (Small *et al.* 2007), a reduction in the air permeability of all produced MDFs as a result of density increasing was observed. The air permeability of B2 and B3 MDFs decreased by 12.8% and 31.6% compared with that of control MDF, respectively. The barrier performance of Na⁺MMT nanoclay improves with increasing nanoclay loading. Indeed, the synergy of increasing amounts of Na⁺MMT nanoclay reduces the air permeability and the exfoliation of clay platelets causes more difficult air permeability through the Na⁺MMT-added MDFs. The nanoparticles create a “tortuous path” within the matrix for the gases to pass (Ray and Okamoto 2003).

Table 4. The air permeability data for 6 groups of MDFsa

Density of board (kg m ⁻³)	Na ⁺ MMT content (%)	Specific permeability (× 10 ⁻¹⁴ m ³ m ⁻¹)
650	0	13.8 (5.95)
	2.5	13.7 (8.81)
	5	13.5 (2.70)
750	0	3.62 (2.22)
	2.5	3.21 (1.87)
	5	2.75 (2.82)

^a Values in parentheses are standard deviations.

Moisture diffusion coefficient

The values of dimensionless diffusivity for all 6 groups of specimens are presented in table 5. The dimensionless diffusivity ranged from 63×10^{-5} to 72×10^{-5} for the MDFs with density of 650 kg m^{-3} and from 45×10^{-5} to 56×10^{-5} for those with density of 750 kg m^{-3} . The mass diffusivity through the Na⁺MMT-added MDFs increased with increasing nanoclay loading. Therefore, the nanoclay doesn't have a suitable effect on the water barrier performance of the MDFs. The hydrophilic nature of the clay makes it hydrophilic (Low *et al.* 2004). Therefore, the moisture diffusion coefficient increased in all MDFs containing nanoclay. Similarly, according to the results obtained by Yano *et al.* (1993), the equilibrium moisture content (EMC) of polyimide/clay nanocomposite was just slightly lower compared to the polyimide matrix but, the gas permeability significantly reduced by means of nanoclay. The mass diffusivity manner is slightly the same as the equilibrium moisture content (EMC). There are three interactions in the structure of our produced MDFs: the interaction of water molecules (moisture) with the hydrophilic nanoclay, the interaction of water molecules with UF resin and the interaction of water molecules with the hydroxyl groups of the wood fibers. The interaction of water with the hydrophilic nanoclay may result to decrease the water barrier performance of the Na⁺MMT-added MDFs.

Table 5. The dimensionless diffusivity for the produced MDFsa

Density of board (kg m ⁻³)	Na ⁺ MMT content (%)	Dimensionless diffusivity (× 10 ⁻⁵)
650	0	63 (9.82)
	2.5	68 (6.94)
	5	72 (14.6)
750	0	45 (10.9)
	2.5	52 (5.71)
	5	56 (7.80)

^a Values in parentheses are standard deviations.

FE-SEM micrograph analysis

Figure 4 shows the FE-SEM micrographs of MDF produced by adding of 5% Na⁺MMT nanoclay in the UF resin. Based on figure 4, nanoclay with a bit agglomeration is observed in the MDF structure. The observations are similar to those for a previous study which evaluated the effects of nanoparticle and matrix interface on the nanocomposites properties (Miller 2008). The micrographs show distinct regions of clay while adjacent regions of the MDF contain little visible nanofiller which might be covered by the resin.

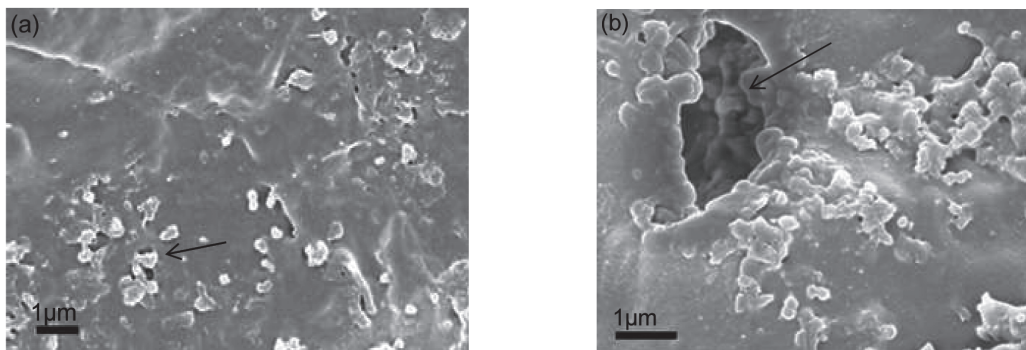


Figure 4. SEM images of MDF produced with a Na⁺MMT nanoclay-added UF resin.

(a) The arrow shows the silicate layers covered by UF resin (10,000 \times)

(b) A pit partially filled by UF resin and silicate layers (15,000 \times). The tiny particles of silicates can decrease the air permeability.

CONCLUSION

Mass transfer properties, including air permeability and mass diffusivity were determined for medium density fiberboard (MDF) reinforced with Na⁺MMT nanoclay. The air permeability through the reinforced MDF decreased by increasing the nanoclay particles. In fact, the slight percentages of Na⁺MMT nanoclay resulted in better air barrier property due to silicate layers of nanoclay. Tortuous path was created as the result of exfoliation and dispersion of nanoclay and subsequently, the flow of air molecules through MDF diminished. SEM images and X-ray diffraction patterns suggested the dispersion and exfoliation of Na⁺MMT in the reinforced MDFs. The moisture absorption of nanoclay-added MDFs was higher than that of control MDF, mainly because of high surface area and hydrophilic nature of nanoclay.

ACKNOWLEDGEMENTS

We would like to give a special thanks to Professor Takashi Nishino from Kobe University for X-ray diffraction and FE-SEM studies. The authors are also thankful to Majid Namdari and Mosayab Dalvand for their general help.

REFERENCES

- Ashori, A.; Nourbakhsh, A. 2009.** Effects of nanoclay as a reinforcement filler on the physical and mechanical properties of wood-based composite. *Journal of composite materials* 43: 1869-1875.
- Campbell, S.; Johnston, J.C.; Ingharm, L.; Mccorcle, L.; Silverman, E. 2003.** Analysis of the barrier properties of polyimide silicate nanocomposites. In: Proceedings of 48th international SAMPE symposium, Mississippi, USA, 1124-1131.
- Faruk, O.; Matuana, L.M. 2008.** Nanoclay reinforced HDPE as a matrix for wood-plastic composites. *Composites Science and Technology* 68: 2073-2077.
- Ganev, S.; Cloutier, A.; Beauregard, R.; Gendron, G. 2005a.** Linear expansion and thickness swell of MDF as a function of panel density and sorption state. *Wood and fiber science* 37: 327-336.
- Ganev, S.; Cloutier, A.; Gendron, G.; Beauregard, R. 2005b.** Finite element modeling of the hygroscopic warping of medium density fiberboard. *Wood and fiber science* 37: 337-354.
- Ghasemi, I.; Kord, B. 2009.** Long-term water absorption behaviour of polypropylene/wood flour/organoclay hybrid nanocomposite. *Iranian Polymer Journal* 18 (9): 683-691.
- Lee, S.Y.; Kang, I.A.; Doh, G.H.; Kim, W.J.; Kim, J.S.; Yoon, H.G.; Wu, Q. 2008.** Thermal, mechanical and morphological properties of polypropylene/clay/wood flour nanocomposites. *Express Polymer Letters* 2 (2): 78-87.
- Lei, H.; Du, G.; Pizzi, A.; Celzard, A. 2008.** Influence of nanoclay on urea-formaldehyde resins for wood adhesives and its model. *Journal of Applied Polymer Science* 109: 2442-2451.
- Lei, Y.; Wu, Q.; Clemons, C.M.; Yao, F.; Xu, Y. 2007.** Influence of nanoclay on properties of HDPE/wood composites. *Journal of Applied Polymer Science* 106: 3958-3966.
- Low, H.Y.; Liu, T.X.; Loh, W.W. 2004.** Moisture sorption and permeation in polyamide 6/clay nanocomposite films. *Polym Int* 53: 1973-1978.
- Miller, S.G. 2008.** Effects of nanoparticle and matrix interface on nanocomposite properties. Ph.D. Thesis, Akron University, Ohio, USA.
- Miller, S.G.; Meador, M.A. 2007.** Polymer-layered silicate nanocomposites for cryotank applications. In: 48th AIAA/ASME/ASCE/AHS/ASC structures, structural dynamics, and materials conference, Honolulu, Hawaii.
- Osman, M.A.; Mittal, V.; Morbidelli, M.; Suter, U.W. 2003.** Polyurethane adhesive nanocomposites as gas permeation barrier. *Macromolecules* 36: 9851-9858.
- Pannirselvam, M.; Genovese, A.; Jollands, M.C.; Bhattacharya, S.N.; Shanks, R.A. 2008.** Oxygen barrier property of polypropylene-polyether treated clay nanocomposite. *Express Polymer Letters* 2 (6): 429-439.
- Parhizkari, M.M.; Taramian, A.; Taghiyari, H.M. 2010.** Tension wood formation in populus nigra and its effects on longitudinal gas permeability under different drying conditions. In: 11th international IUFRO wood drying conference, Skelleftea, Sweden.

Rana, H.T. 2003. Moisture diffusion through neat and glass-fiber reinforced vinyl ester resin containing nanoclay. M.Sc. Thesis, Department of Chemical Engineering, West Virginia University, USA.

Ray, S.S.; Okamoto, M. 2003. Polymer/layered silicate nanocomposites: a review from preparation to processing. *Prog. Polym. Sci* 28: 1539-1641.

Rousset, P.; Perre, P.; Girard, P. 2004. Modification of mass transfer properties in poplar wood (*Populus*) by a thermal treatment at high temperature. *Holz Roh Werkst* 62: 113-119.

Shi, S.H.Q. 2007. Diffusion model based on Fick's second law for the moisture absorption process in wood fiber-based composites: is it suitable or not? *Wood Sci Technol* 41: 645-658.

Siau, J.F. 1995. *Wood: Influence of moisture on physical properties*. Department of wood science and forest products, Virginia Polytechnic Institute and State University, USA.

Small, C.H.M.; McNally, G.M.; Mcshane, P.; Kenny, I. 2007. Polypropylene/styrene-ethylene-butylene-styrene thermoplastic elastomer nanocomposite films. *Journal of Vinyl and Additive Technology* 13: 46-52.

Sorz, J.; Hietz, P. 2006. Gas diffusion through wood: implications for oxygen supply. *Trees* 20: 34-41.

Southern Clay Product Inc. 2010. Cloisite® Na⁺ Typical Physical Properties Bulletin. http://www.scpod.com/product_bulletins/PB%20Cloisite%20NA+.pdf. (available in October 2010).

Straze, A.; Gorisek, Z. 2006. Drying characteristics of compression wood in norway spruce (*Picea abies* Karst). *Wood Structure and Properties* 6: 399-403.

Tarmian, A.; Perre, P. 2009. Air permeability in longitudinal and radial directions of compression wood of *Picea abies* L. and tension wood of *Fagus sylvatica* L. *Holzforschung* 63 (3): 352-356.

Taylor, R.E.; Butzelaar, P.; Leeuwen, G.V.; Keyes, J.; Gimenez, C.H.; Macdonald, B. 2009. Global MDF rising capacity, declining operating rates. *Wood Markets* 14 (8): 1-2.

Walther, T.; Thoemen, H.; Terzic, K.; Meine, H. 2006. New opportunities for the microstructural analysis of wood fiber networks. In: Proceedings of the tenth European panel products symposium, Llandudno, Wales, UK, 23-32 pp.

Wegner, T.H.; Jones, P.H.E. 2006. Advancing cellulose-based nanotechnology. *Cellulose* 13: 115-118.

Wegner, T.H.; Winandy, J.E.; Ritter, M.A. 2005. Nanotechnology opportunities in residential and non-residential construction. In: 2nd International Symposium on Nanotechnology in Construction, Bilbao, Spain.

Yano, K.; Usuki, A.; Okada, A.; Kurauchi, T.; Kamigaito, O. 1993. Synthesis and properties of polyimide-clay hybrid. *J Polym Sci Part A: Polym Chem* 31: 2493-2498.

Zeng, Q.H.; Yu, A.B.; Lu, G.Q.; Paul, D.R. 2005. Clay-based polymer nanocomposites: research and commercial development. *Journal of Nanoscience and Nanotechnology* 5: 1574-1592.